Journal of Brilliant Engineering 1 (2026) 41102
Brilliant Engineering
journal home: www.acapublishing.com/journals/4/ben

Research Article

Electrospun PVDF/GO/CNT Composite Nanofiber Membranes for Efficient Adsorption of Methylene Blue from Aqueous Solutions

Efekan Karadağ[1], Zafer Ekinci[*,2]
[1,2]Department of Chemical Engineering, Atatürk University, Erzurum, Türkiye

Keywords

Adsorption,
Graphene oxide,
PVDF composite,
Carbon nanotube,
Nanofiber membrane
Electrospun membrane.

Abstract

Electrospun PVDF/GO/CNT nanofiber membranes were produced and evaluated as adsorbents for the removal of methylene blue (MB) from water. Adsorption tests were carried out in batch mode and the effects of pH, contact time, initial concentration, membrane dosage, and temperature were examined. The uptake showed a clear dependence on pH, with the highest performance obtained near pH 8. Under the representative conditions (C_0 = 100 mg L^{-1}, V = 100 mL, m = 0.03 g, 25 °C, 60 min), the membrane adsorbed about 280 mg g^{-1}, corresponding to roughly 84% removal. Equilibrium was reached within approximately one hour, and subsequent experiments were conducted at 25 °C. The kinetic data were fitted satisfactorily by the pseudo-second-order model; however, this model is used only as a fitting tool and not as proof of a specific rate-controlling mechanism. Among the equilibrium models tested, the Freundlich equation provided the best description of the data, indicating adsorption on a heterogeneous surface. Thermodynamic evaluation yielded negative ΔG° values and a positive ΔH° (46.7 kJ mol^{-1}), showing that the process is spontaneous and endothermic within the studied temperature range. In contrast to studies that examine only PVDF/GO or PVDF/CNT systems, the present work investigates the combined use of GO and CNT in a single electrospun membrane and shows that their coexistence enhances MB uptake. These findings suggest that the PVDF/GO/CNT membrane is a workable material for MB removal from aqueous solutions.

1. Introduction

The rapid growth of industrial production has led to a substantial rise in the release of dye-containing effluents into aquatic ecosystems. Among different manufacturing sectors, textile, leather, paper, and dyeing facilities are recognized as major contributors because they rely heavily on synthetic colorants [1]. These compounds usually possess complex aromatic rings, strong chemical stability, and high resistance to biological degradation, which makes their removal from water particularly challenging [2]. Even at very low concentrations, dyes can limit light transmission in water bodies, suppress photosynthesis, and cause toxic effects in aquatic organisms and humans [3].

Methylene blue (MB) is one of the most widely used cationic dyes, commonly employed in textile finishing, printing, and several biomedical applications. Owing to its solubility and aromatic structure, MB persists in aqueous environments and is not easily eliminated by conventional treatment processes [4]. Exposure to water contaminated with MB has been linked to various health problems, including respiratory complications, methemoglobinemia, and cellular damage [5]. Therefore, MB is frequently selected as a model contaminant when evaluating new adsorbent materials [6].

A wide range of technologies — coagulation, flocculation, biological processes, membrane filtration, and advanced oxidation — have been explored for dye removal [7]. Nevertheless, many of these methods suffer from drawbacks such as high operating costs, sludge formation, secondary pollution, or limited effectiveness for highly stable dye molecules. By comparison, adsorption is considered attractive because it is simple to operate, efficient over a broad concentration range, and allows adsorbent reuse [8]. The overall efficiency of adsorption systems is primarily dictated by the surface chemistry, functional groups, and interaction mechanisms of the chosen adsorbent.

Over the last decade, polymer-based nanofiber membranes have attracted increasing attention as promising adsorbents owing to their high surface-area-to-volume ratio, interconnected porosity, and adjustable surface properties [9]. Polyvinylidene fluoride (PVDF) is widely preferred in membrane technology due to its combination of mechanical strength and chemical and thermal stability [10]. Electrospinning enables PVDF to be converted into porous fibrous mats with controllable morphology and high porosity [11]. However, its inherently hydrophobic nature limits adsorption performance, underscoring the need for surface modification or the incorporation of functional nanofillers.

Graphene oxide (GO), a two-dimensional carbon material rich in oxygen-containing groups, can interact with dye molecules through electrostatic attraction, hydrogen bonding, and π–π interactions [12]. Carbon nanotubes (CNTs) also exhibit a high affinity for aromatic species and can enhance the reactivity of composite surfaces [13]. When GO and CNTs are incorporated together into a polymer matrix, several studies have reported synergistic behavior, leading to improved dispersion, more accessible active sites, and enhanced adsorption performance relative to single-filler systems [14].

Electrospinning provides an efficient means of uniformly distributing GO and CNTs within PVDF fibers, yielding porous structures with multiple adsorption sites [15]. Despite the growing number of reports on PVDF/GO and PVDF/CNT composites, investigations of the combined role of both

*Corresponding Author: zekinci@atauni.edu.tr
Received 22 Dec 2025; Revised 07 Jan 2026; Accepted 07 Jan 2026
https://doi.org/10.36937/ben.2026.41102

fillers in electrospun PVDF membranes for MB removal remain limited. In particular, more detailed studies are needed to clarify adsorption mechanisms, kinetic behavior, isotherm characteristics, and thermodynamic aspects in such ternary systems.

In the present work, we propose that co-incorporating one-dimensional CNTs and two-dimensional GO within the PVDF matrix forms a complementary network. CNTs may function as spacers preventing the restacking of GO sheets, while GO can anchor CNTs and reduce their aggregation. This cooperative interaction is expected to promote filler dispersion, increase the number of available adsorption sites, and consequently enhance MB uptake.

To evaluate this concept, electrospun PVDF/GO/CNT composite nanofiber membranes were produced and tested for MB adsorption from aqueous solution. The effects of pH, contact time, initial dye concentration, and temperature were systematically examined. Kinetic, equilibrium, and thermodynamic analyses were conducted to elucidate the adsorption mechanism and support the development of efficient composite membranes for dye-contaminated waters.

Furthermore, the complementary roles of the two fillers were considered: GO introduces oxygen-containing functionalities that enhance electrostatic and hydrogen-bonding interactions, whereas CNTs provide π–π interactions and mechanical reinforcement. Studying both additives within a single electrospun membrane helps clarify how their combined presence influences dye removal. In contrast to many earlier works that used either GO or CNT alone, this study focuses on a ternary PVDF/GO/CNT membrane. It examines the synergistic effect of both carbon-based additives on the adsorption performance.

2. Materials and Methods

2.1. Materials

Polyvinylidene fluoride (PVDF, Sigma-Aldrich, ≥99%, Mw ≈530000) was used as the polymer matrix for membrane fabrication. Graphene oxide (GO, Nanografi) and multi-walled carbon nanotubes (CNT, Nanografi, 96%) were employed as functional nanofillers. MB (Sigma-Aldrich, ≥97%) was selected as a model cationic dye for adsorption studies. Deionized water was used in all experimental procedures.

2.2. Preparation of PVDF/GO/CNT Composite Spinning Solution

The PVDF/GO/CNT composite nanofiber membranes were produced by electrospinning. The preparation of the spinning solution was carried out in several stages. First, the polymer matrix was prepared, after which graphene oxide and carbon nanotubes were dispersed separately and finally combined with the polymer solution to obtain a homogeneous mixture.

A PVDF concentration of 10% (w/v) was targeted. For this purpose, 2.00 g of PVDF was dissolved in 10 mL of DMF at 60 °C. Following the subsequent addition of the GO and CNT dispersions, the total volume of the spinning dope reached 20 mL, so that the final PVDF concentration remained 10% (w/v).

GO and CNTs were then incorporated as reinforcing additives. In the final spinning solution, both GO and CNTs were present at 0.5% (w/v), corresponding to approximately 5 wt% relative to the PVDF mass. In practice, this was achieved by dispersing 0.10 g of each filler into the 20 mL solution.

The GO and CNT dispersions were first treated ultrasonically and then added dropwise to the PVDF solution while stirring. The resulting mixture was allowed to homogenize for about 1–2 h before electrospinning. During this period, the viscosity of the spinning solution was periodically checked to ensure that it remained within a workable range (approximately 850–1500 cP). Viscosity measurements were carried out using an Anton Paar SVM 3001 Smart Viscometer (Anton Paar, Austria) at 25 ± 1 °C, and each value represents the mean of three independent measurements.

2.3. Electrospinning of PVDF/GO/CNT Nanofiber Membranes

Electrospinning was performed using a stainless-steel needle (22 gauge) at 18 kV, with a distance of 15 cm between the needle tip and collector. The experiments were carried out at room conditions (23 ± 2 °C; relative humidity 40–45%). A stationary flat aluminum collector was employed, and electrospinning was continued for approximately four hours to obtain continuous nanofiber mats. The resulting membranes had an average thickness of 120 ± 10 μm, determined from five random measurements with a digital micrometer. After collection, the membranes were dried under vacuum at 60 °C for 24 h to remove residual DMF before adsorption tests.

2.4. Characterization

The morphology of the nanofiber membranes was examined by scanning electron microscopy (SEM, Zeiss Sigma 300). Elemental mapping and qualitative assessment of GO and CNT distribution were performed using energy-dispersive X-ray spectroscopy (EDS). Fourier-transform infrared spectroscopy (FTIR, Bruker VERTEX 70v) was recorded over the range 4000–400 cm^{-1} to identify characteristic functional groups and possible interactions within the composite.

2.5. Determination of Point of Zero Charge

The point of zero charge (pHpzc) of the PVDF/GO/CNT membrane was determined by the pH-drift method. A set of 0.01 mol L^{-1} NaCl solutions (100 mL) with initial pH values ranging from 2 to 10 was prepared. To each solution, 0.03 g of membrane was added, and the suspensions were shaken at 150 rpm for 24 h. The pHpzc was defined as the pH at which no net change in pH was observed between the initial and final pH values.

2.6. Batch Adsorption Experiments

Batch adsorption tests were conducted by adding 0.03 g of membrane to 100 mL MB solutions with initial concentrations of 100–250 mg L^{-1}. The pH was adjusted to values between 3 and 9 using dilute acid or base. Experiments were carried out at 25, 30, 35, and 40 °C under agitation at 150 rpm.

At predetermined time intervals (0–120 min), aliquots were withdrawn and analyzed by UV–visible spectrophotometry (Optizen ⍺) at 664 nm. The adsorption capacity (q_t), adsorption equilibrium capacity (q_e), and removal efficiency (%) were calculated using Equations (1), (2), and (3) [16].

$$q_t = \frac{C_0 - C_t}{m} V \quad (1)$$

$$q_e = \frac{C_0 - C_e}{m} V \quad (2)$$

$$\text{Removel } (\%) = \frac{C_0 - C_e}{C_0} 100 \quad (3)$$

where q_t and q_e (mg g^{-1}) represent the adsorption capacity at time t (min) and at equilibrium, respectively. C_0, C_t, and C_e (mg L^{-1}) are the initial, time-dependent, and equilibrium MB concentrations. m (g) is the adsorbent mass and V (L) is the solution volume. All adsorption experiments were carried out in triplicate, and average values are reported.

3. Results and Discussion

3.1. Morphological and Elemental Characterization

As shown in Figure 1a, the SEM micrographs of pristine PVDF nanofibers display a uniform, bead-free, and randomly oriented network, which is consistent with stable jet formation during electrospinning.

After the addition of GO and CNT, the composite membrane (Figure 1b) still exhibits a continuous nanofibrous morphology. A modest increase in both fiber diameter and surface roughness is observed, suggesting that the nanofillers were incorporated without disrupting fiber formation.

EDS analysis of the pristine PVDF fibers (Figure 1a) reveals signals corresponding to C, O, and F, with approximate weight fractions of 52.88 wt% C, 5.14 wt% O, and 41.98 wt% F. In the PVDF/GO/CNT composite (Figure 1b), the carbon and oxygen contents increase to 72.32 wt% and 8.76 wt%, respectively, whereas the fluorine content decreases to 18.92 wt%. These shifts are consistent with the introduction of GO and CNT, which contribute carbon- and oxygen-rich species to the fiber surface.

It should be emphasized that EDS provides semi-quantitative information and probes mainly the near-surface region (typically a few hundred nanometers). Therefore, the pronounced reduction in the fluorine signal does not necessarily imply a substantial dilution of PVDF throughout the entire fiber. Instead, it likely reflects preferential enrichment of GO and CNT at the outer surface (“skin layer”), while PVDF remains the dominant constituent within the fiber core. This surface enrichment is beneficial for adsorption, as it increases the density of accessible functional groups and π-electron sites involved in dye interaction.

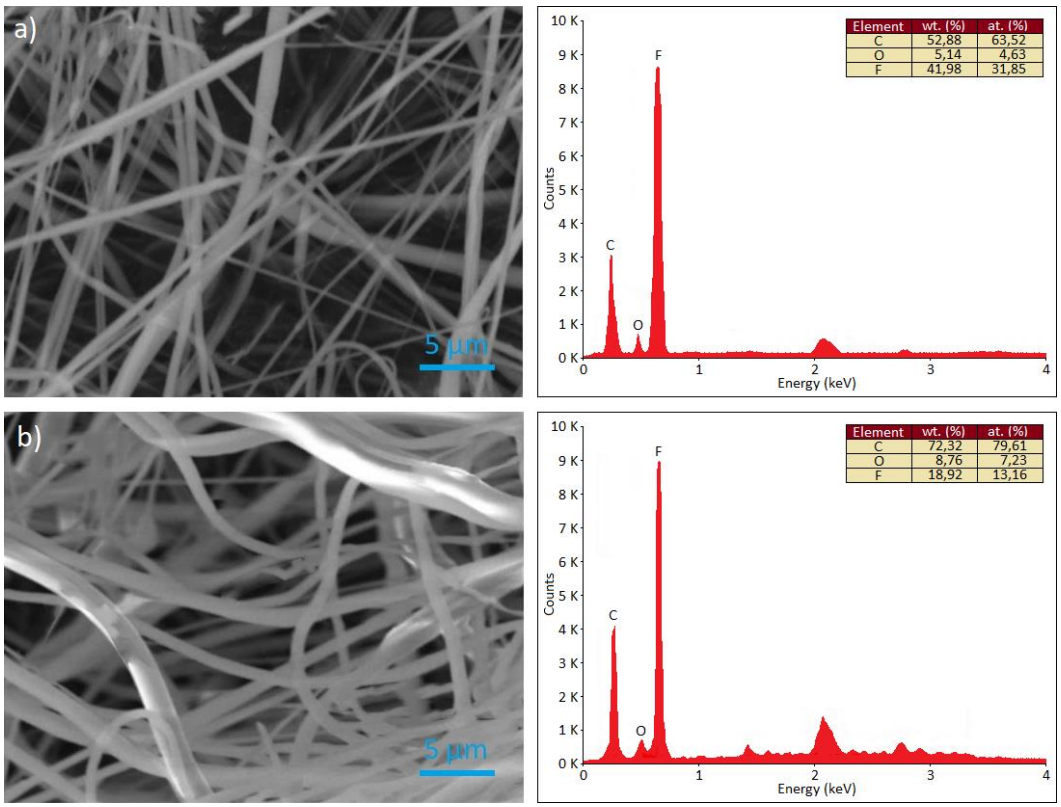

Figure 1. SEM images and corresponding EDS spectra of electrospun nanofiber membranes: (a) pristine PVDF nanofibers and (b) PVDF/GO/CNT composite nanofibers

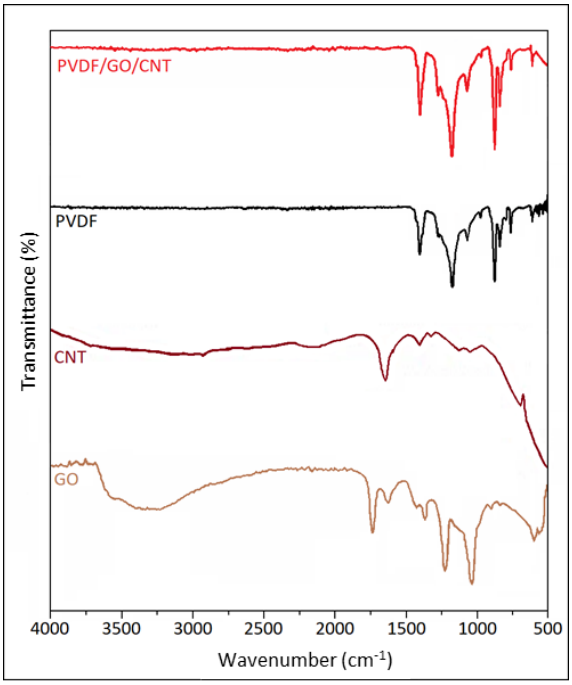

Figure 2. FTIR spectra of graphene oxide (GO), carbon nanotubes (CNT), pristine PVDF, and PVDF/GO/CNT composite nanofiber membranes.

Figure 2 presents the FTIR spectra of GO, CNT, pristine PVDF, and the PVDF/GO/CNT composite membranes. In the GO spectrum, a broad band in the 3400–3200 cm^{-1} region is associated with O–H stretching, while the peak near 1720 cm^{-1} is assigned to C=O stretching. The band at approximately 1620 cm^{-1} corresponds to C=C stretching, and additional features between 1220 and 1050 cm^{-1} are attributable to C–O–C and C–O vibrations. Taken together, these bands are consistent with the presence of oxidized oxygen functionalities typical of graphene oxide.

The FTIR spectrum of CNTs shows only weak, broad absorptions. A small band near 1600 cm^{-1} (C=C stretching) and features in the 1200–1000 cm^{-1} range can be discerned, which reflects the low IR activity of graphitic carbon with limited surface functionalization.

For pristine PVDF, several characteristic absorption bands are clearly visible. The band at 840 cm^{-1}, commonly associated with the β-phase of PVDF, appears alongside the C–F stretching band near 1275 cm^{-1} and multiple bands in the 1400–1000 cm^{-1} interval related to C–H and C–F vibrations. These features are consistent with PVDF's semi-crystalline structure.

In the PVDF/GO/CNT composite, the FTIR spectrum largely preserves PVDF's characteristic peaks but shows noticeable changes in relative intensities and slight peak shifts. A modest enhancement of the band at 840 cm^{-1} suggests that the incorporation of GO and CNT may influence chain polarization and favor the formation of electroactive conformations. Weak signals attributable to oxygen-containing groups derived from remain detectable, indicating that these functionalities persist after electrospinning. Small shifts observed in the 1000–1300 cm^{-1} region is likely due to physical interactions between PVDF chains and the embedded nanofillers rather than to the formation of new chemical bonds.

The point of zero charge (pHpzc) of the PVDF/GO/CNT composite membrane determined by the pH-drift method is shown in Figure 3.

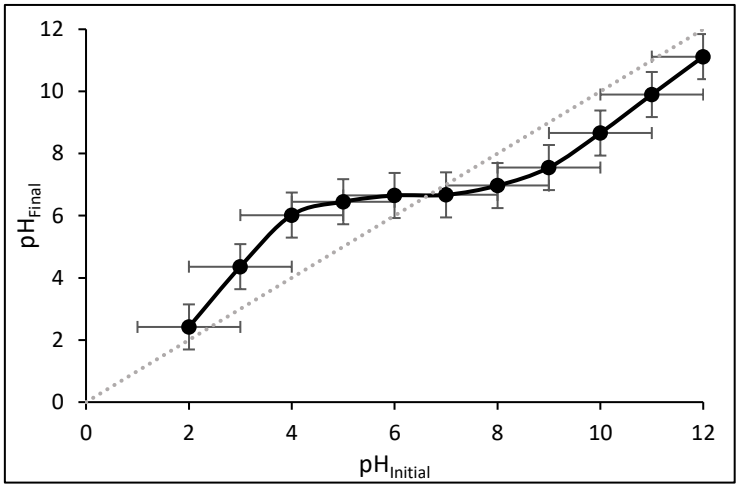

Figure 3. Determination of pH_{pzc} value of PVDF/GO/CNT composite membrane

The pH_{pzc} of the PVDF/GO/CNT membrane was found to be approximately 6.65, corresponding to the point at which the initial and final pH values coincide. Below this value, the membrane surface is expected to carry a net positive charge, whereas above 6.65 it becomes predominantly negative. Such a change in surface charge directly influences the adsorption of cationic dyes like methylene blue, as electrostatic attraction becomes more favorable at pH values above the pH_{pzc}.

The pH_{pzc} obtained indicates that the composite membrane can interact efficiently with MB under neutral to slightly alkaline conditions. At higher pH, however, partial dimerization of MB, together with competition from hydroxide ions, may limit overall uptake despite the favorable electrostatics.

The influence of solution pH on MB adsorption by the PVDF/GO/CNT membrane is presented in Figure 4.

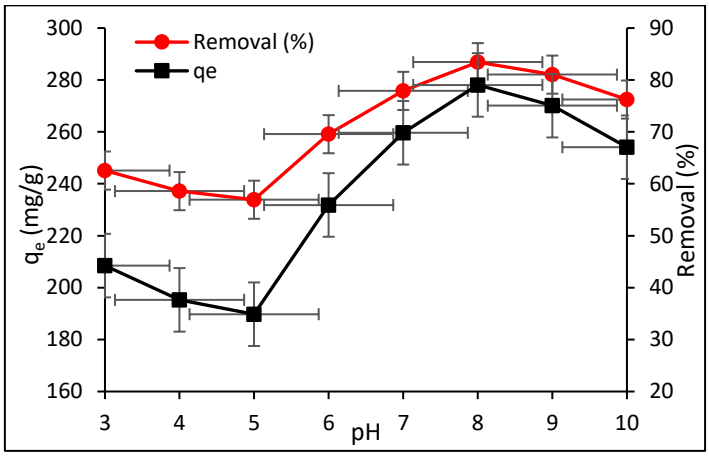

Figure 4. Effect of pH change on MB q_e and removal efficiency of the composite membrane (T=25°C, C_0=100 mg/L, m=30 mg)

Both the adsorption capacity (q_e) and the removal efficiency showed a clear dependence on solution pH. Under acidic conditions (pH 3–5), lower adsorption capacities were observed, with q_e values below about 200 mg g^{-1} and removal efficiencies of 60–65%. This behavior can be explained by the membrane's predominantly positive surface charge at low pH, which reduces electrostatic attraction to the cationic MB molecules.

As the pH increased from 6 to 8, a marked improvement in adsorption performance was observed. The adsorption capacity rose steadily and reached its maximum near pH 8, where an equilibrium capacity of approximately 280 mg g^{-1} and a removal efficiency of about 85% were recorded. This optimal pH is consistent with the measured pHpzc (~6.65), above which the membrane surface becomes negatively charged, favoring electrostatic interactions with MB.

At higher pH values (pH 9–10), a slight decrease in both q_e and removal efficiency was observed. This decline may be associated with partial saturation of available sites and possible competition effects in highly alkaline media, including interactions with hydroxide ions and dye aggregation.

The effects of contact time and adsorbent dosage on MB uptake by the PVDF/GO/CNT membrane are presented in Figure 5.

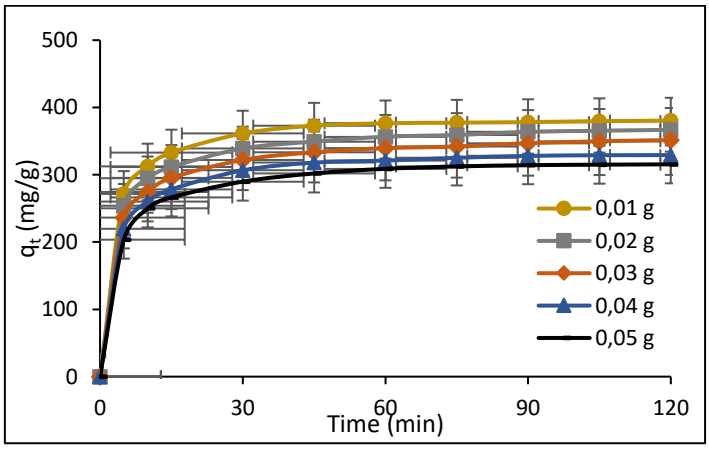

Figure 5. Effect of adsorbent dosage on the q_t of MB by the composite membrane (T=25°C, C_0=200 mg/L, pH=8)

For all tested adsorbent dosages (0.01–0.05 g), a rapid increase in q_t was observed during the initial adsorption stage. This behavior is attributed to the abundance of readily accessible active sites on the membrane surface at the beginning of the process.

With increasing contact time, the adsorption rate progressively decreased, and q_t tended toward a plateau, indicating that equilibrium conditions were approached. For every dosage examined, equilibrium was reached after approximately 60 min, beyond which no appreciable increase in uptake occurred. In this study, equilibrium was assumed when the relative change in q_t over 30 min was below 2 %, a criterion satisfied at 60 min under all conditions. Accordingly, 60 minutes was selected as the contact time for subsequent experiments.

Although somewhat higher adsorption capacities were obtained at lower dosages, a dosage of 0.03 g was chosen for the remaining tests because it provided stable and reproducible adsorption behavior while maintaining measurable removal efficiencies.

The influence of the initial MB concentration on the adsorption performance of the PVDF/GO/CNT composite membrane is shown in Figure 6 and summarized in Table 1.

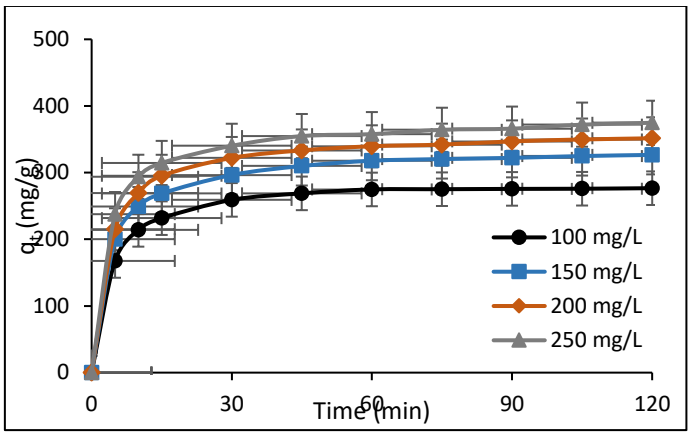

Figure 6. Effect of initial MB concentration on the q_t of the composite membrane (T=25°C, m=30 mg, pH=8)

Table 1. Mass balance verification for MB adsorption experiments

Experiment No	C_0 (mg L^{-1})	C_e (mg L^{-1})	V (L)	m (g)	q_e (mg g^{-1})	Removal (%)
1	100	16.36	0.1	0.03	278.8	≈ 84
2	150	51.42	0.1	0.03	328.6	≈ 66
3	200	93.89	0.1	0.03	353.7	≈ 53
4	250	136.93	0.1	0.03	376.9	≈ 45

For all investigated initial concentrations (100–250 mg L^{-1}), a rapid rise in q_t occurred during the early stage of adsorption, followed by a gradual approach to a steady value. This trend suggests that a large number of readily accessible adsorption sites were initially available on the membrane surface.

With increasing dye concentration, the adsorption capacity increased accordingly. At an initial concentration of 100 mg L^{-1}, q_t reached about 275 mg g^{-1}, whereas higher values of approximately 325, 350, and 375 mg g^{-1} were obtained at 150, 200, and 250 mg L^{-1}, respectively. The observed increase in q_t with concentration is attributed to the larger concentration gradient, which enhances the driving force for mass transfer of MB molecules toward the adsorbent surface.

Equilibrium was reached within approximately 60 min across all concentrations tested, indicating that the time required to attain steady-state uptake was not strongly dependent on the initial dye concentration. The highest uptake occurred at 250 mg L^{-1}; beyond this level, further capacity increases are expected to be limited by progressive saturation of adsorption sites rather than by external mass-transfer constraints. Accordingly, 250 mg L^{-1} was selected as the representative concentration for subsequent analyses.

The influence of temperature on MB adsorption by the PVDF/GO/CNT composite membrane is presented in Figure 7.

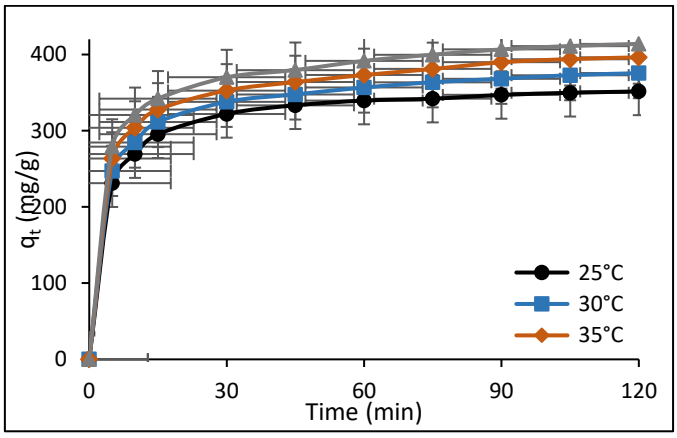

Figure 7. Effect of temperature on the q_t of the composite membrane (C_0=200 mg/L, m=30 mg, pH=8)

For all investigated temperatures (25–40 °C), a rapid rise in q_t was observed at the beginning of the process, after which the curves gradually approached a steady value. This behavior is consistent with fast uptake on readily accessible surface sites during the early stages of adsorption.

An increase in temperature led to a modest yet apparent increase in adsorption capacity. At 25 °C, the uptake at equilibrium was approximately 350 mg g^{-1}, while slightly higher values of about 370, 395, and 410 mg g^{-1} were obtained at 30, 35, and 40 °C, respectively. The observed trend

can be attributed to improved molecular mobility at higher temperatures and to thermodynamically more favorable interactions between MB molecules and the active sites on the composite membrane.

Equilibrium was attained within about 60 min for all tested temperatures, suggesting that the characteristic time to reach steady uptake was not strongly temperature-dependent. Although adsorption capacity increased with temperature, the additional gain beyond ambient conditions was relatively small. Since efficient uptake was already observed at 25 °C, this temperature was used as the reference condition for most subsequent experiments.

Adsorption isotherm models were then applied to interpret the equilibrium data and to gain insight into the surface characteristics of the PVDF/GO/CNT membrane. In this study, the Langmuir, Freundlich, and Temkin models were evaluated, and their linearized forms, along with the fitted parameters, are presented in Table 2.

Table 2. The equations and constants of isotherm models

Isotherm Model	Equation	Constants	References
Langmuir	$\frac{1}{q_e} = \frac{1}{q_e K_L C_e} + \frac{1}{q_{max}}$	q_{max}: the capacity of maximum adsorption K_L: the constant of the isotherm	
Freundlich	$\log q_e = \log K_F + \frac{1}{n} \log C_e$	K_F: the constant of isotherm n: the intensity of adsorption	[16]
Temkin	$q_e = B_T \ln K_T + B_T \ln C_e$ $B_T = \frac{RT}{b}$	R: the universal gas constant (8.314 J/mol.K) T: the temperature (K) b: the isotherm constant about the adsorption heat K_T: the constant of equilibrium binding	

The adsorption experiments used for isotherm analysis were designed to describe the equilibrium behavior of MB on the PVDF/GO/CNT composite membrane. All measurements were performed at 25 °C and pH 8, using 0.03 g of membrane in 100 mL of solution. Initial MB concentrations ranged from 100 to 250 mg L^{-1}, and the suspensions were agitated at 150 rpm. Equilibrium was reached within approximately 60 min, and the corresponding equilibrium data were used for model fitting.

The applicability of the Langmuir, Freundlich, and Temkin models was assessed using the equilibrium data. The calculated parameters and correlation coefficients are listed in Table 3, and the fitted curves are shown in Figure 8.

Among the models examined, the Freundlich model provided the best statistical agreement with the experimental data ($R^2 \approx 0.998$). This result suggests that the membrane surface does not behave as a perfectly uniform adsorbent and that adsorption sites with different affinities may be present. Such behavior is reasonable given the combined contributions of the PVDF, GO, and CNT domains in the composite structure.

The Langmuir separation factor RLR_LRL was found to fall between 0 and 1 over the studied concentration range, indicating favorable adsorption conditions. In addition, the Freundlich exponent n>1 reflects a generally favorable uptake process; however, this parameter should be interpreted cautiously, as it does not on its own distinguish between physisorption and chemisorption.

The Temkin isotherm also provided an acceptable description of the data. The positive Temkin constant B_T indicates that the heat of adsorption decreases gradually with coverage, a typical feature of heterogeneous systems. The obtained Temkin parameter b (51.3 kJ mol^{-1}) is of the same order of magnitude as the enthalpy change derived from the Van't Hoff plot (ΔH° = 46.7 kJ mol^{-1}). This consistency supports the overall thermodynamic interpretation, although the values should be viewed as approximations because they depend on the definition of the equilibrium constant and on the assumptions inherent to each model.

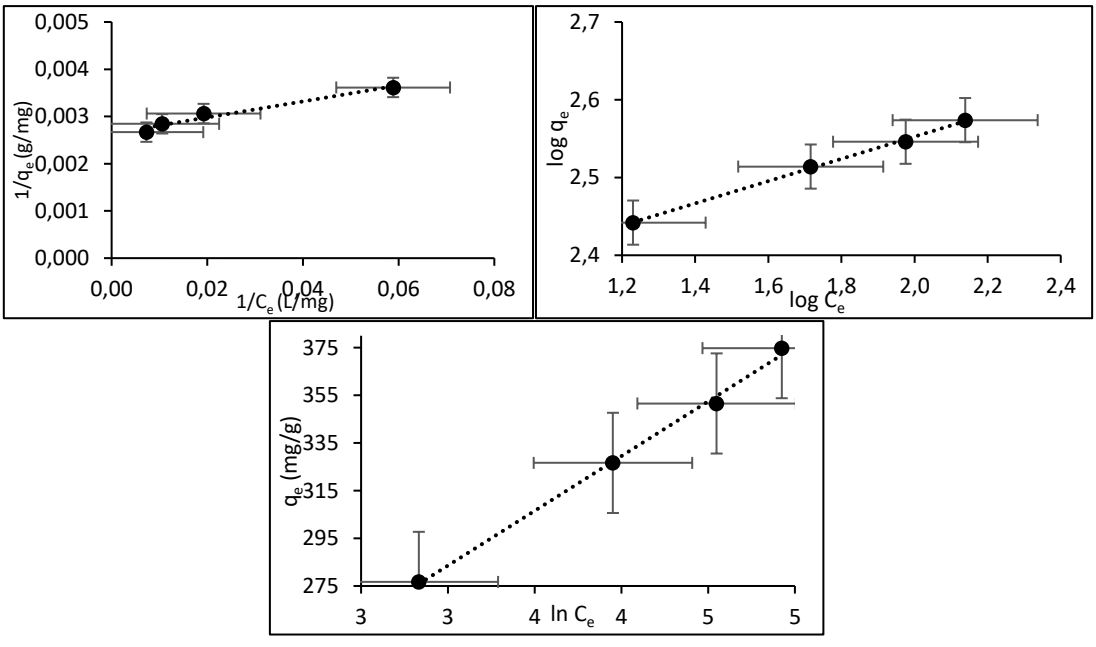

Figure 8. The adsorption isotherms graphs of a) Langmuir, b) Freundlich, and c) Temkin models (m=30 mg, pH=8, t=60 min)

Table 3. Isotherm constants for MB adsorption onto the PVDF/GO/CNT composite membrane (m=30 mg, pH=8, t=60 min)

Isotherm	**Isotherm Constants**				**R^2**
			R_L		
			0.076	(100 mg/L)	
Langmuir	q_{max} (mg/g)	K_L (L/mg)	0.052	(150 mg/L)	0.972
	363.4	0.172	0.039	(200 mg/L)	
			0.015	(250 mg/L)	
Freundlich	K_F (mg/g)	n (g/L)			0.996
	187.3	7.0			
Temkin	B_T	K_T (L/g)	b (kJ/mol)		0.987
	47.6	25.2	51.3		

Adsorption kinetics provides insight into how rapidly equilibrium is approached and which steps may limit the overall rate. In the present study, the kinetic behavior of MB uptake by the PVDF/GO/CNT composite membrane was analyzed using three commonly applied models: the pseudo-first-order, pseudo-second-order, and intra-particle diffusion models. These models were used to examine how well the experimental time-dependent data could be described and to obtain indicative kinetic parameters. The corresponding linear equations and fitted parameters are listed in Table 4.

It should be noted that the models were fitted in their linearized forms, which may introduce bias into the estimated parameters. Therefore, the kinetic parameters reported here are primarily intended for comparative purposes rather than as definitive mechanistic proof.

Table 4. The equations and constants of kinetic models

Kinetic Model	Equation	Constants	References
Pseudo-First-Order	$\ln(q_e - q_t) = \ln q_e + k_1 t$	k_1 = the rate constant	
Pseudo-Second-Order	$\frac{t}{q_t} = \frac{1}{k_2 q_e^2} + \frac{t}{q_e}$	k_2 = the rate constant	[17]
Intra-Particle Diffusion	$q_t = k_{id} t^{\frac{1}{2}} + C$	k_{id}: the constants of Intraparticle diffusion C: a constant	

The adsorption experiments used for kinetic analysis were performed under the same conditions employed in the isotherm studies (C_0 = 100–250 mg L^{-1}, membrane dosage = 0.03 g, V = 100 mL, pH = 8, and T = 25 °C) to maintain consistency and allow direct comparison of the results. Time-dependent adsorption data obtained under these conditions were used to evaluate the kinetic behavior of MB uptake by the PVDF/GO/CNT composite membrane.

The kinetic parameters calculated from the pseudo-first-order, pseudo-second-order, and intra-particle diffusion models, together with the corresponding correlation coefficients, are summarized in Table 5. The fitted curves for each model are shown in Figure 9. All kinetic measurements were carried out in triplicate, and the mean values were used for model fitting.

Table 5. Kinetic model constants for MB adsorption onto the PVDF/GO/CNT composite membrane (T=25°C, m=30 mg, pH=8, t=60 min)

Kinetic Model	Initial Concentration (mg L^{-1})	Kinetic Model Constants	R^2
Pseudo-First-Order	100	0.0375 min^{-1}	0.877
	150	0.0364 min^{-1}	0.945
	200	0.0359 min^{-1}	0.943
	250	0.0341 min^{-1}	0.929
Pseudo-Second-Order	100	0.00112 g mg^{-1} min^{-1}	0.995
	150	0.00083 g mg^{-1} min^{-1}	0.994
	200	0.00080 g mg^{-1} min^{-1}	0.994
	250	0.00075 g mg^{-1} min^{-1}	0.993
Intra-Particle Diffusion	100	10.4 g mg^{-1} $min^{0.5}$	0.759
	150	12.3 g mg^{-1} $min^{0.5}$	0.954
	200	13.0 g mg^{-1} $min^{0.5}$	0.801
	250	12.9 g mg^{-1} $min^{0.5}$	0.820

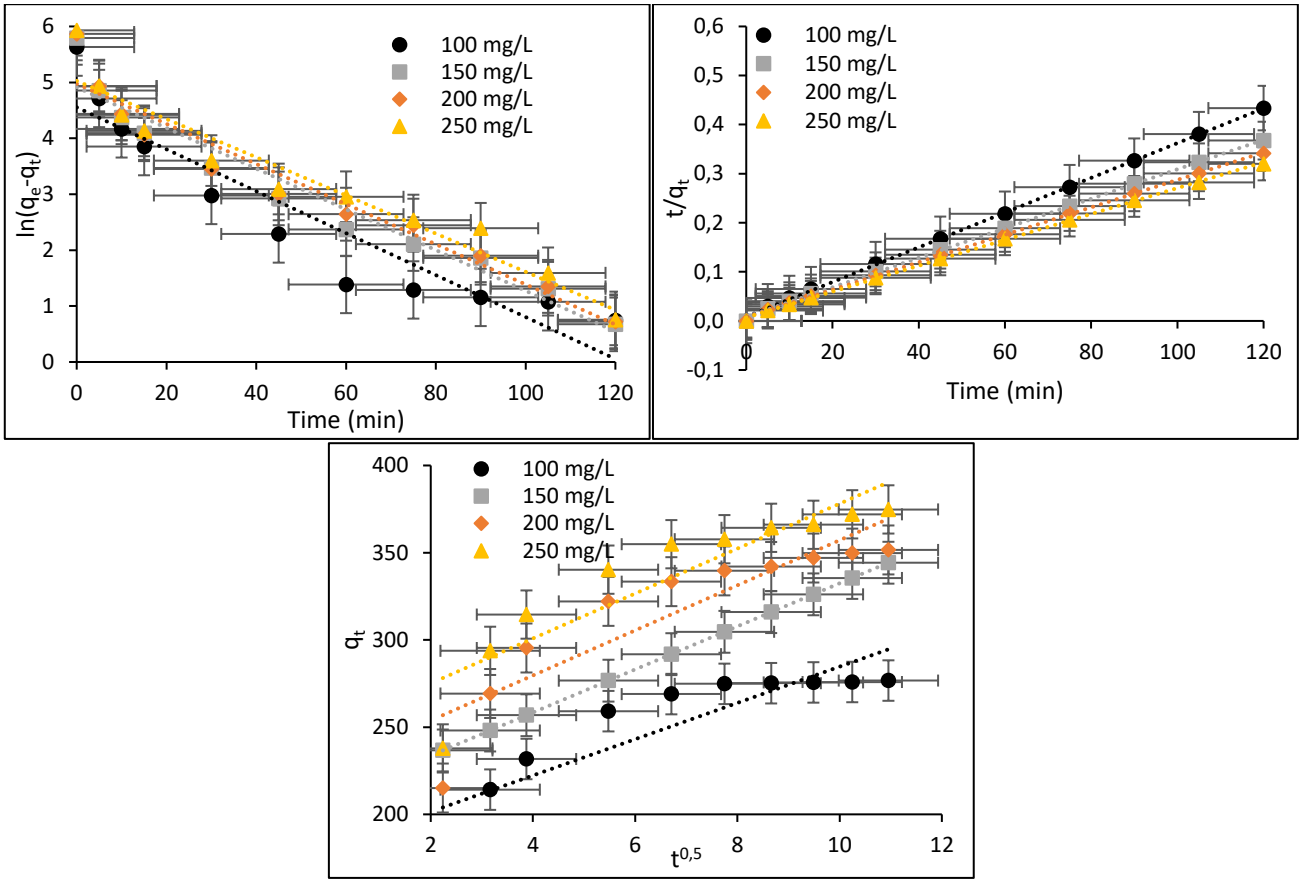

Figure 9. Kinetic model fitting curves for MB adsorption onto the PVDF/GO/CNT composite membrane: (a) pseudo-first-order, (b) pseudo-second-order, (c) intra-particle diffusion models (T=25°C, m=30 mg, pH=8, t=60 min)

The suitability of the kinetic models was initially assessed by comparing their correlation coefficients (R^2). The pseudo-first-order model yielded relatively low R^2 values (0.877–0.945), indicating a limited ability to describe the adsorption process over the investigated concentration range. The intra-particle diffusion model produced more scattered correlation coefficients (0.759–0.954). Moreover, the corresponding plots did not pass through the origin, implying that intra-particle diffusion contributes to the adsorption process but does not control it as the sole rate-limiting step. A contribution from boundary-layer (film) diffusion is therefore also likely.

In contrast, the pseudo-second-order (PSO) model gave the highest and most consistent correlation coefficients (R^2 = 0.993–0.995) for all initial MB concentrations, indicating that PSO provides the best empirical description of the time-dependent adsorption data. The PSO rate constant k2k_2k2 decreased from 0.00112 to 0.00075 g mg^{-1} min^{-1} as the initial dye concentration increased, which may be attributed to increased competition among MB molecules for available adsorption sites.

It should be emphasized that the models were fitted in their linearized forms, which can bias parameter estimates. Accordingly, the kinetic parameters are interpreted here primarily for comparison rather than as definitive mechanistic proof. Although the PSO model fits the data well, it remains an empirical model; therefore, the results suggest an essential contribution from surface-controlled steps but do not exclude parallel mass-transfer phenomena such as intra-particle diffusion.

Thermodynamic parameters of the adsorption process were subsequently evaluated using equilibrium data obtained at different temperatures. The standard Gibbs free energy change (ΔG°) was calculated using Equations (4) and (5), whereas the enthalpy (ΔH°) and entropy (ΔS°) changes were derived from the Van't Hoff relationship in Equation (6).

$$\Delta G^0 = -RT \ln K_C \quad (4)$$

$$K_C = K_C^* x \frac{m}{V} \text{ and } K_C^* = \frac{q_e}{C_e} \quad (5)$$

$$\ln K_C = -\frac{\Delta H^\circ}{RT} + \frac{\Delta S^\circ}{R} \quad (6)$$

The thermodynamic behavior of MB adsorption onto the PVDF/GO/CNT composite membrane was evaluated using the Van't Hoff approach. Equilibrium data obtained at 25, 30, 35, and 40 °C were used to calculate the thermodynamic parameters (Figure 10). The distribution constant K_c was defined as the ratio of the equilibrium concentration of adsorbed dye to that remaining in solution. It was converted into a dimensionless form before thermodynamic evaluation. The resulting values of ΔG°, ΔH°, and ΔS° are summarized in Table 6.

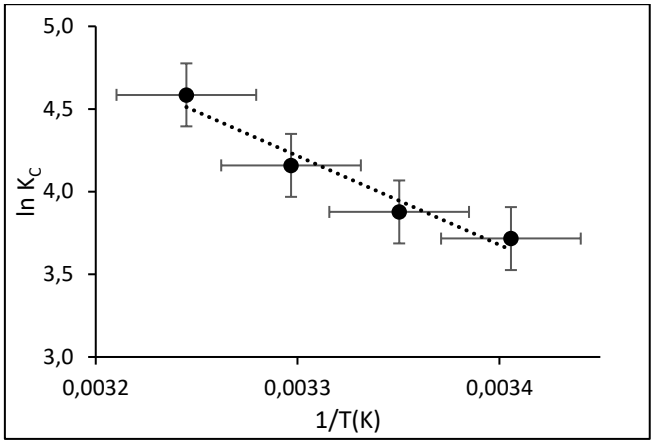

Figure 10. Van't Hoff plot for MB adsorption onto the PVDF/GO/CNT composite membrane (C_0=200 mg/L, m=30 mg, pH=8, t=60 min)

Table 6. Thermodynamic parameters for MB adsorption onto the PVDF/GO/CNT composite membrane (C_0=200 mg/L, m=30 mg, pH=8, t=60 min)

Temperature (°C)	ΔG°(kJ/mol)	ΔH°(kJ/mol)	ΔS° (kJ/mol K)	R^2
25	-10.58	46.7	0.192	0.962
30	-12.67			
35	-16.59			
40	-25.72			

The standard Gibbs free energy change (ΔG°) values were negative at all studied temperatures (25–40 °C), indicating that the adsorption process is thermodynamically favorable within this range. In addition, the magnitude of ΔG° became slightly more negative as temperature increased, suggesting that adsorption is facilitated to some extent at higher temperatures.

The positive enthalpy change (ΔH° = 46.7 kJ mol^{-1}) is consistent with an endothermic process and agrees with the observed increase in adsorption capacity with temperature. The positive entropy change (ΔS° = 0.192 kJ mol^{-1} K^{-1}) implies an increase in overall disorder at the solid–solution interface during adsorption, which may arise from partial release of structured water molecules and possible rearrangements of surface species.

The Van't Hoff plot yielded a satisfactory linear correlation (R^2 = 0.962), suggesting that the calculated thermodynamic parameters are internally consistent with the equilibrium data. Taken together, these results indicate that MB adsorption onto the PVDF/GO/CNT composite membrane is a favorable and predominantly endothermic process, with entropic contributions also playing a role.

4. Conclusion

In this study, electrospun PVDF/GO/CNT composite nanofiber membranes were prepared and examined as adsorbents for the removal of methylene blue from aqueous solution. The incorporation of graphene oxide and carbon nanotubes resulted in nanofibrous mats with good structural integrity, and the presence of carbon-based additives was confirmed by SEM, EDS, and FTIR analyses. The introduction of oxygen-containing functionalities and π-electron-rich domains is expected to contribute to dye–surface interactions.

Batch adsorption experiments showed that solution pH, contact time, initial dye concentration, and temperature noticeably affected MB uptake. Under the tested conditions, pH 8 provided the highest measured uptake (≈ 284 mg g^{-1}) with a removal efficiency of about 85%. Equilibrium was reached within approximately 60 min, indicating relatively rapid adsorption. Although the adsorption capacity increased slightly with temperature, appreciable removal was already achieved at 25 °C, which was used as the reference condition.

Kinetic modelling indicated that the pseudo-second-order expression gave the best empirical fit to the time-dependent data. In contrast, intra-particle diffusion appeared to contribute without acting as the sole controlling step. Equilibrium data were more consistent with the Freundlich isotherm than with the Langmuir isotherm, suggesting the presence of adsorption sites with different affinities. Thermodynamic analysis yielded negative ΔG° values and a positive ΔH° (46.7 kJ mol^{-1}), consistent with a predominantly endothermic process driven by entropic contributions.

Taken together, these results indicate that the PVDF/GO/CNT composite membrane shows promising adsorption performance toward methylene blue under relatively mild operating conditions. Further work addressing regeneration, long-term stability, and performance in more complex water matrices would help clarify its potential for practical water and wastewater treatment applications.

Declaration of Conflict of Interests

The authors declare no conflicts of interest. They have no known competing financial interests or personal relationships that could have appeared to influence the work reported in this paper.

References

[1.] Crini, G., Non-conventional low-cost adsorbents for dye removal: A review. *Bioresource Technology* 97 (2006) 1061–1085.

[2.] Gupta, V.K., Suhas, Application of low-cost adsorbents for dye removal – A review. Journal of Environmental Management 90 (2009) 2313–2342.

[3.] Slama, H.B., Chenari Bouket, A., Pourhassan, Z., Alenezi, F.N., Silini, A., Cherif-Silini, H., Oszako, T., Luptakova, L., Dye pollution in water and wastewater: Sources, impacts and treatment methods. Environmental Chemistry Letters 19 (2021) 373–404.

[4.] Arias, E., Carro, L., Sanchez, M., Removal of methylene blue from aqueous solution using adsorption processes. Journal of Water Process Engineering 36 (2020) 101264.

[5.] Bužga, M., Koubová, M., Lapčík, L., Toxicological effects of methylene blue and its environmental implications. Chemosphere 286 (2022) 131747.

[6.] Oladoye, P.O., Bamigboye, M.O., Adeniyi, A.G., Methylene blue removal using advanced adsorbent materials: A review. Environmental Technology & Innovation 25 (2022) 102150.

[7.] Vasiljević, T., Novaković, D., Maletić, S., Dye wastewater treatment by conventional and advanced methods: A comparative review. Separation and Purification Technology 310 (2023) 123072.

[8.] Yousef, R.I., El-Eswed, B., Al-Muhtaseb, A.H., Adsorption characteristics of dyes onto modified adsorbents. Chemical Engineering Journal 390 (2020) 124507.

[9.] Al-Abduljabbar, A., Farooq, U., Nanofiber-based membranes for dye adsorption applications. Journal of Environmental Chemical Engineering 11 (2023) 109463.

[10.] Boo, C., Lee, J., Elimelech, M., Omniphobic nanofibrous membranes for water treatment. Journal of Membrane Science 518 (2016) 97–109.

[11.] Haider, A., Haider, S., Kang, I.K., A comprehensive review on electrospinning of nanofibers. Arabian Journal of Chemistry 11 (2018) 1165–1188.

[12.] Bagri, A., Mattevi, C., Acik, M., Chabal, Y.J., Chhowalla, M., Structural evolution during the reduction of chemically derived graphene oxide. Journal of Physical Chemistry C 114 (2010) 12053–12061.

[13.] Aqel, A., El-Nour, K.M.M.A., Ammar, R.A.A., Al-Warthan, A., Carbon nanotubes, science and technology part I. Arabian Journal of Chemistry 5 (2012) 1–23.

[14.] Chae, H.R., Kim, J., Yoon, J., Synergistic effect of graphene oxide and carbon nanotubes in polymer composite membranes. Composites Part B 222 (2021) 109073.

[15.] Lei, T., Zhao, J., Zhou, C., Surface-modified PVDF nanofiber membranes fabricated by electrospinning. Applied Surface Science 357 (2015) 1162–1169.

[16.] Kızıltaş, H., Production of highly effective adsorbent from tea waste, and its adsorption behaviors and characteristics for the removal of Rhodamine B. International Journal of Environmental Analytical Chemistry 104 (2022) 1730–1749.

[17.] Kızıltaş, H., Orange G'nin sulu çözeltilerden uzaklaştırılması için α-Fe_2O_3 nanopartiküllerinin adsorban olarak kullanılması: Adsorpsiyon, kinetik ve termodinamik özellikleri. Avrupa Bilim ve Teknoloji Dergisi 21 (2021) 43–52.

How to Cite This Article

Karadağ, E., Ekinci, Z., Electrospun PVDF/GO/CNT Composite Nanofiber Membranes for Efficient Adsorption of Methylene Blue from Aqueous Solutions, Brilliant Engineering, 1(2026), 41102.
https://doi.org/10.36937/ben.2026.41102